Journal of Applied Polymer Science

The Crystallization Morphology Evolution of Polyoxymethylene/Poly(ethylene oxide) Blend Micropart Prepared under Microinjection Molding Conditions

Changbin Tan, Shibing Bai, Qi Wang
State Key Laboratory of Polymer Materials Engineering, Polymer Research Institute, Sichuan University, Chengdu 610065, People's Republic of China
Correspondence to: Q. Wang (E-mail: qiwang@scu.edu.cn)

ABSTRACT: This article is the first study on the microinjection molding and the effects of the microprocessing parameters on the crystallization and orientation of polyoxymethylene/poly(ethylene oxide) (POM/PEO) blend, which has better toughness and self-lubricity compared with the neat POM and therefore is a better candidate material for making microparts like microgears with higher performances. The crystalline and phase morphologies were investigated by polarized light microscope (PLM), differential scanning calorimeter (DSC) and scanning electron microscope (SEM). The crystalline orientation of the microparts was evaluated by two-dimensional wide-angle X-ray diffraction (2D-WAXD) and Herman's orientation function. The experimental results showed that both POM and POM/PEO microparts prepared by microinjection molding exhibited three distinct layers, i.e., skin layer, shear layer and core layer, while the latter had thicker shear layer but thinner skin layer and core layer. PEO was well dispersed in POM matrix. The spherulite size, the melting point as well as the crystallinity of POM in the POM/PEO blend decreased due to the interference of PEO in the crystallization of POM. A shish-kebab structure was observed in the shear layers of the POM/PEO microparts. The effects of processing parameters on the thicknesses of different layers of the POM/PEO microparts were investigated. With increase of the injection speed or decrease of the mold temperature, the skin layer and the core layer became thicker, while the shear layer and the oriented region became thinner. However, the influence of the injection pressure was not obvious. Also, the processing parameters affected the crystalline orientation of the POM/PEO microparts. With increase of the injection speed or decrease of the mold temperature, the orientation function f decreased, indicating a lower degree of orientation. © 2014 Wiley Periodicals, Inc. J. Appl. Polym. Sci. **2014**, *131*, 40538.

KEYWORDS: blends; morphology; thermoplastics

Received 14 October 2013; accepted 31 January 2014
DOI: 10.1002/app.40538

INTRODUCTION

With the development of the modern industry, the miniaturized products or microparts have been increasingly applied in many fields such as optical communications, image transfer, biochemical medicine, information storage, precision machinery, and so on.[1] Microparts generally have one of the following features,[2] weights in milligrams or featured dimensions in micrometers. It has been a big challenge to manufacture microparts with high precision, high performance, low cost, and high productivity.

Compared with the microparts made of nonpolymer materials such as metals, silicon, and glass, the polymer microparts have the advantages such as easy manufacturing, low cost, multifunction, etc., and have developed very fast in recent years. Among the processing methods used to make polymer-based microparts, microinjection molding (μIM) is the most attractive technology due to its high efficiency, low cost, and good precision, etc.[3] Many polymeric microparts, such as micro-heat exchangers, micropumps, biochips, optical grating elements, etc., have been successfully fabricated by microinjection molding.[4]

Like the conventional injection molding, the structure and properties of microparts made by μIM are also strongly affected by the microprocessing conditions. However, according to the definition of micropart, the micropart should have the weight, dimension or microstructure which is much smaller than that of the macropart prepared by the conventional injection molding. This surely would make the μIM essentially different from the conventional injection molding. The essential difference can be that due to the substantial reduction in the runner and cavity size, relative to the conventional injection molding, the μIM

process has extremely high injection speed (1200 mm s^{-1} vs. 100 mm s^{-1}), extremely high shear rate ($>10^7$ s^{-1}), much higher temperature gradient (much more rapid cooling rate) and extremely short filling time. As a result, most polymer microinjection moldings are conducted in the extreme processing conditions. Under such a stringent condition, some polymer materials may suffer decomposition, incomplete filling of the cavity or poor dimensional stability of micropart. Undoubtedly, there should be a much higher requirement for the polymer materials to be microprocessed than those processed by conventional injection molding. In addition, the rheological behavior of μIM can be also very different from the one described by conventional rheology's laws. It has been reported that the wall-slip effects would occur in the channels with size of several micrometers or less and would become more significant when the microchannel size further decreases.[4–6] These special processing conditions play a significant role in controlling the crystallization behaviors and morphology of the prepared micropart. Therefore, investigation of the relationship between processing parameters and crystallization behavior is not only very meaningful for ultimate application of polymeric materials but also very useful to predict and understand the property change of microparts under microinjection molding conditions.[7]

The crystalline morphology and orientation of semicrystalline polymers have proved to show a significant impact on their physical properties (mechanical, optical, electrical, chemical etc.).[7–10] However, the study of μIM of polymeric materials mainly focuses on mold technology, special machine, replication quality analysis, numerical simulation etc.,[11] and the investigation on the crystalline morphology and orientation of microparts in μIM is relatively limited, most of which were on polypropylene,[7–9] while other polymeric materials (single component, blend, hybrid or composite) are rarely involved.[5]

Polyoxymethylene (POM) is an important engineering thermoplastic and commonly used to manufacture microparts such as microgears, micropumps, microfluidic devices, etc.[12] For microgears, however, its lubricity and toughness should be improved because the friction coefficient and abrasion wear of POM increases rapidly under the high load and high sliding speed,[13] and the quite large spherulites of POM make it very sensitive to notch and a low notched impact strength.[14]

In our previous work, we found that poly(ethylene oxide) (PEO) could be used to improve the toughness and lubricity of POM. Because as polyethers, POM [—$(CH_2$—O$)_n$—] and PEO [— $(CH_2$—CH_2—O$)_n$—], have similar chemical structure, small difference in solubility parameter ($\triangle\delta \approx 0.6$), and most interesting and importantly, their molecular chains could be included in each other due to their special conformation ($H9_5$ for POM and $H7_2$ for PEO, the size and shape can induce such inclusion, which may be regarded as a new type of intermolecular complexation).[15–19] All these would make POM/PEO a compatible blend and have better toughness and lubricity compared to neat POM. Our previous experimental results confirmed that the introduction of PEO can remarkably increase the notched impact strength and elongation at the break and also decrease the friction coefficient of POM. At a PEO content of 5 wt % and M_n of 500,000, the toughness of the blend was enhanced by 100%, the friction coefficient was decreased to 35% that of POM, while the strength and Young's modulus almost kept unchanged.[15,17] Obviously, the POM/PEO blend is a better candidate material than neat POM to manufacture microgears with higher performances.

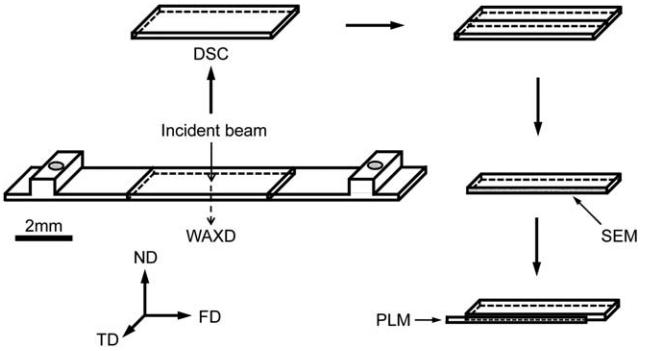

Figure 1. Schematic drawing of sampling methods of microparts for WAXD, DSC, SEM and PLM analyses FD: flow direction, TD: transverse direction, ND: normal direction.

Although numerous studies on μIM of polymeric materials have been reported in recent years, most still focused on neat polymers, and few on the polymer blends or composites,[20–22] which can be expected to endow the microparts with multi-functions and higher performances.

This article studied the microinjection molding of the POM/PEO crystalline/crystalline polymer blend, investigated the crystallization and orientation of POM/PEO blend microparts under microprocessing conditions using optical, thermal, and X-ray diffraction measurements. The influences of different microinjection molding conditions including injection speed, mold temperature and injection pressure on the crystallization behavior and crystalline orientation of POM/PEO blend micropart were investigated for the first time.

EXPERIMENTAL

Materials

POM (M90), with 80,000–100,000 average molecular weight and 9.0 g/10 min melt flow index (190°C/2.16 kg), was purchased from Yuntianhua, China. PEO with M_n of 500,000 was supplied by Shanghai Jichen Chemical Industry, China.

Sample Preparation

Blends with various compositions of 95/5, 90/10, 80/20, 70/30, and 50/50 in weight ratio of POM to PEO were well mixed and extruded in a parallel twin-screw extruder with screw diameter of 16 mm and the length-to-diameter ratio of 40 : 1 (Thermo Electron GmbH, Germany). The barrel temperatures of each zone from hopper to die were from 155 to 190°C and the screw speed was fixed at 50 rpm.

The POM and POM/PEO (95/5, by wt %) blend microparts were microinjection molded on a Battenfeld MicroPower 5 machine (Wittmann Battenfeld GmbH, Austria). A schematic diagram of the micropart in this study, with the thickness of 280 μm, is shown in Figure 1. The main part of the micropart

Table I. The Microprocessing Parameters Corresponding to Sample Series A, B, and C

Sample series	Injection speed (mm s^{-1})	Mold temperature (°C)	Injection pressure (MPa)	Melt temperature (°C)	Holding pressure (MPa)
A	300–700	50	200	190	80
B	300	30–70	200	190	80
C	300	50	150–250	190	80

was a rectangular geometry, with dimension of 14.8 × 2.9 × 0.28 mm^3, weight of a few milligrams. The rib regions on both sides of the micropart (the circular area in Figure 1) were designed as the positions where the ejector pin contacted, which had the better resistance to contact deformation and damage than the thinner regions in case the micropart was deformed or damaged by the ejector pin when ejected from the mold.

To analyze the influence of the microprocessing parameters, in the same series of experiments, we just changed one processing parameter while fixing the other processing parameters. The microparts prepared with different parameters in a group were labeled A (different injection speeds), B (different mold temperatures), and C (different injection pressures). The processing parameters corresponding to A, B, and C samples are listed in Table I.

Polarized Light Microscope (PLM) Observation

POM and POM/PEO microparts were observed by using 10-μm-thick microtomed cuts. Assuming that the weak variations within results can be caused by their positioning, the sampling zones of the microparts were located in the middle of the micropart, as shown in Figure 1, where the flow is unidirectional.[23] The cross sections were sampled to observe the crystalline morphology along the thickness. The reference mark is given accordingly using FD as representative of the flow direction, TD as representative of the transverse direction and ND as representative of the normal direction, respectively. PLM observations along the TD direction were performed using a DM2500p microscope (Leica Camera AG, Germany) with 90° cross-polarized light, connected with a PL-A662 Pixelink digital camera. The averaged thicknesses of the different layers of samples were adopted by using ten measurements. The measurements were performed using Nano Measurer image analysis software from Fudan University (Shanghai, China).

Melt Flow Index (MFI) Measurements

Melt flow index (MFI) of POM, PEO and the POM/PEO blends was measured by using a CS-127 melt indexer (Custom Scientific Instruments, USA) according to ASTM D1238. A load of 2.16 kg and temperature at 190°C was used in this measurement.

Differential Scanning Calorimeter (DSC) Analysis

The melting behaviors of the samples were determined by Q20 differential scanning calorimeter (TA Instruments, USA) at a heating rate of 10°C min^{-1} from 0 to 200°C under nitrogen atmosphere. To compare the morphological differences between each sample, the sampling zones of the microparts were located in the middle of the micropart, with a weight of ~5 mg, as shown in Figure 1. From heating scans, the melting points of both POM and PEO components could be determined. Moreover, on the basis of the heat of fusion of 100% crystalline POM (317.9 J g^{-1})[24] and PEO (203 J g^{-1}),[25] the crystallinities of both POM and PEO components were calculated.

Scanning Electron Microscope (SEM) Observation

To better characterize the crystalline and phase morphologies which are not very clear in PLM observations, the cryogenically

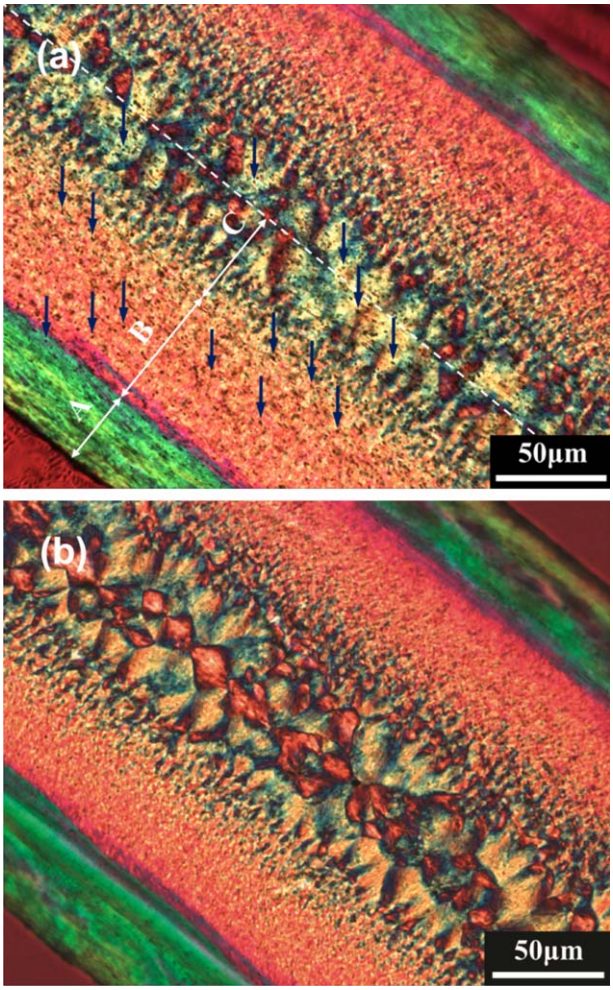

Figure 2. Comparison of the polarized optical micrographs of the full cross-sections of the POM/PEO (a) and pure POM (b) microparts (sample thickness 280 μm) microinjection molded under the same microprocessing conditions (injection speed: 300 mm s^{-1}; mold temperature: 50°C; injection pressure: 200 MPa). [Color figure can be viewed in the online issue, which is available at wileyonlinelibrary.com.]

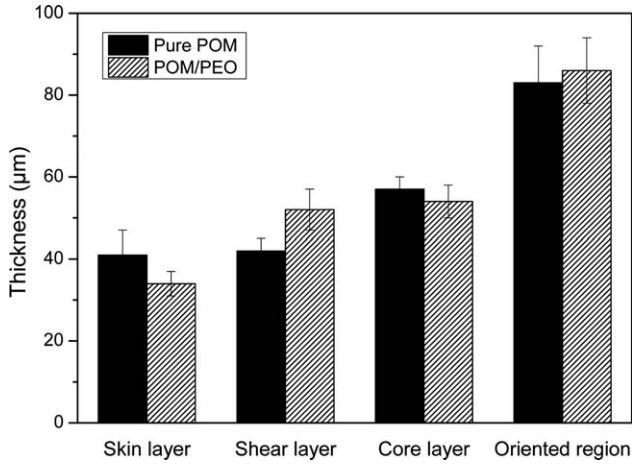

Figure 3. The thicknesses of different layers of pure POM and POM/PEO microparts prepared under the same microprocessing conditions.

fractured samples were first etched in a hexafluoroisopropanol (HFIP) solution and then immersed in distilled water for 24 h at room temperature. After dried under air atmosphere, the etched samples were observed along the TD direction using a high-resolution Inspect F scanning electron microscope (FEI Company, USA) operated at 5 kV. The surfaces of the samples were coated with an Au-Pd nanolayer. The sampling zones of the microparts were the same as above PLM observations, as shown in Figure 1.

Synchrotron Two-dimensional Wide-Angle X-ray Diffraction

Flow-induced oriented structures in the microparts were analyzed by recording 2D-WAXD patterns. The 2D-WAXD experiments were carried out at room temperature on the BL16B1 beamline in the Shanghai Synchrotron Radiation Facility (SSRF), China. The wavelength used is 0.124 nm and the sample-to-detector distance was 110.9 mm. The 2D-WAXD patterns were recorded every 60 s by a Mar165 CCD X-ray detector system. The samples were placed with the orientation (flow direction) perpendicular to the beams. All the 2D-WAXD patterns given in this study have been background corrected and analyzed with Fit2D software from European Synchrotron Radiation Facility. From the 2D-WAXD patterns, azimuthal sections (i.e., scattered intensity as a function of azimuthal angle) of the (100) reflection of hexagonal crystal of POM were obtained to monitor the level of orientation of the (100) crystal plane. To allow a qualitative comparison between different samples, the sampling zones of the microparts were located in the middle of the micropart where the flow is unidirectional, as shown in Figure 1.

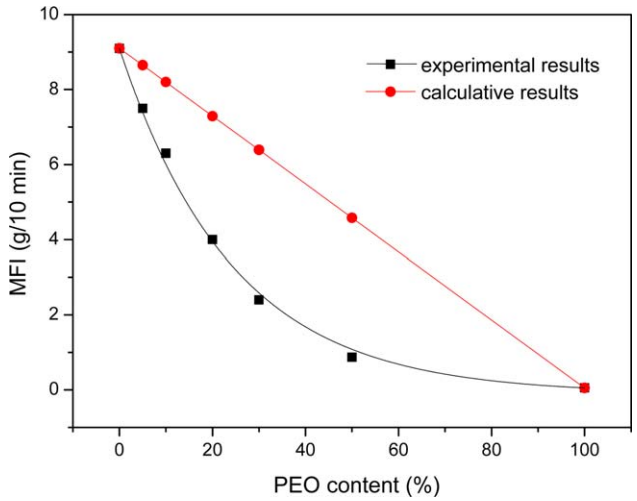

Figure 4. MFI of POM, PEO, and POM/PEO blends. [Color figure can be viewed in the online issue, which is available at wileyonlinelibrary.com.]

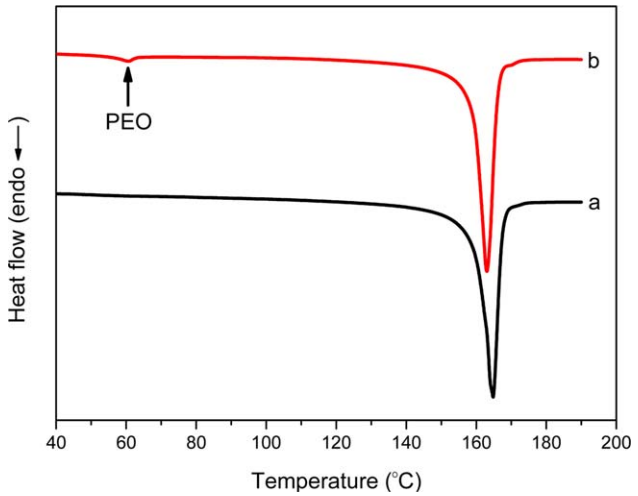

Figure 5. DSC curves of pure POM (a) and POM/PEO (b) microparts prepared under the same microprocessing conditions. [Color figure can be viewed in the online issue, which is available at wileyonlinelibrary.com.]

RESULTS AND DISCUSSION

Effect of PEO Incorporation on Crystalline Morphology

POM/PEO blend is a novel crystalline/crystalline polymer system, as we previously reported. The incorporation of PEO remarkably improved the lubrication performance and impact strength of POM.[15,17] So, it is interesting to investigate the structure changes of POM/PEO blend under microinjection processing conditions so as to prepare microparts (e.g., microgear) with good comprehensive performances. Figure 2 compares the polarized light micrographs of POM/PEO blend micropart and POM micropart. As can be seen, POM/PEO micropart [Figure 2(a)] showed a typical skin-core structure. This skin-core morphology of POM/PEO micropart in fact included three distinct layers across the thickness direction, which can be distinguished clearly by the different colors: A—a

Table II. The Crystallization Parameters of Pure POM and POM/PEO Microparts Prepared under the Same Microprocessing Conditions Obtained from Figure 5

Sample	$T_{m\text{-POM}}$ (°C)	$\triangle H_m$ (J g^{-1})	$X_{c\text{-POM}}$ (%)	$T_{m\text{-PEO}}$ (°C)	$X_{c\text{-PEO}}$ (%)
Pure POM	164.8	161.3	50.7	-	-
POM/PEO	163.1	158.5	49.8	59.4	43.6

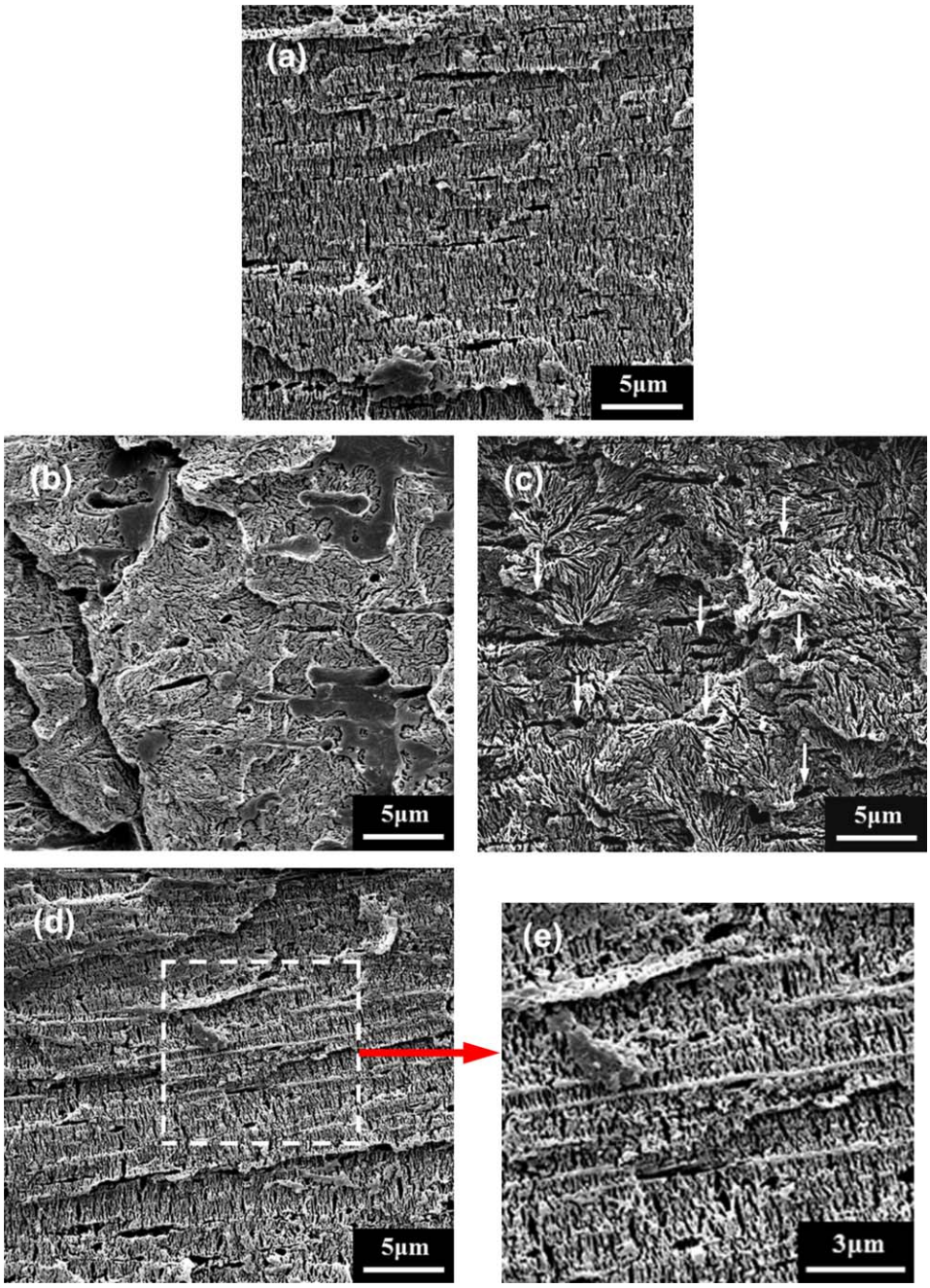

Figure 6. SEM micrographs of the skin layer (a), core layer (b* and c) and shear layer (d and e) of the POM/PEO micropart prepared under the microinjection molding conditions of injection speed 300 mm s^{-1}, mold temperature 50°C and injection pressure 200 MPa. *Figure 6(b) is the SEM image before etching and the other photos are the ones after etching. [Color figure can be viewed in the online issue, which is available at wileyonlinelibrary.com.]

thin and oriented skin layer near the mold wall [the green zone in Figure 2(a)]; B—an oriented nonspherulitic zone [shear layer, the red zone in Figure 2(a)]; C—a spherulitic core region without orientation (core layer). It seems that in the core layer appeared fine asymmetric spherulites, asymmetric oblate spherulites and randomly nucleated spherulites in an order from the surface to the center.

Many investigations[23,26,27] showed that the skin-core structure, particularly the involved oriented region (including both the skin layer and the shear layer), determined the mechanical properties (the tensile strength, Young's modulus, impact toughness, etc.) of the injection molded parts to a considerable degree. So, it is interesting and important to investigate the distribution of the different layers in the polymer micropart. For pure POM, the similar skin-core morphology was also found [Figure 2(b)]. However, some morphological differences existed between POM and POM/PEO microparts due to the presence of PEO. First of all, the PEO phase [the dark dot-like parts in

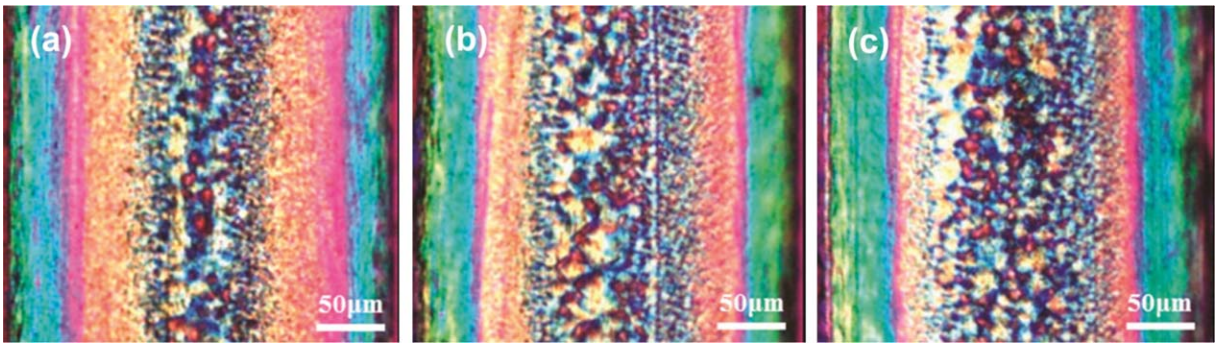

Figure 7. Polarized light micrographs of the full cross-sections of the POM/PEO microparts prepared at different injection speeds: (a) 300 mm s^{-1}, (b) 500 mm s^{-1}, and (c) 700 mm s^{-1}. [Color figure can be viewed in the online issue, which is available at wileyonlinelibrary.com.]

Figure 2(a) indicated by the arrow] was uniformly dispersed in POM matrix. The PEO dispersed phase in POM matrix showed a "sea–island" morphology. Moreover, the approximately spherical PEO domain showed a size smaller than 2 μm. Second, compared with pure POM micropart, the shear layer thickness of POM/PEO micropart increased, while the corresponding skin layer thickness decreased, as shown in Figure 2. To conduct a quantitative comparison of thickness of each layer, the thicknesses of different layers and the oriented region were measured and shown in Figure 3. Considering the total thicknesses of different samples were almost the same, the measured value of the thickness of different layer rather than the relative value (relative to the total sample thickness) was used. It can be seen that the thickness of the shear layer was about 52 μm for the POM/PEO micropart and 42 μm for the POM micropart, respectively. The contrary trend was found in the skin layer, i.e., the thickness of the skin layer was 34 μm for the POM/PEO micropart and 41 μm for the POM micropart, respectively. Therefore, the oriented region of the POM/PEO micropart (86 μm) was only slightly thicker than that of the POM micropart (83 μm). Above changes might be ascribed to an increase in the melt viscosity due to the introduction of PEO, which increased the relaxation time and accordingly promoted the formation of the shear layer.[23] To confirm this, the melt flow index measurements on the POM/PEO blends with different PEO contents (all the measurements were based on the same raw material POM and PEO) were conducted, as shown in Figure 4. The experimental results showed that the addition of PEO increased the melt viscosity obviously (decrease in MFI). With increase of the PEO content, the MFI value remarkably decreased and was even lower than the calculated one. The changes were attributed to the special interactions between POM and PEO macromolecules due to the chain inclusion or entanglement induced by their special chain conformation ($H9_5$ for POM and $H7_2$ for PEO, respectively, matching each other in both spacial size and shape), as explained in our previous papers.[16–19] Although in the microinjection molding process the actual shear rate is possibly much higher than that occurring in the MFI testing process, it is believed that there are still the interactions existing between POM and PEO macromolecular chains, which can possibly lead to the viscosity of the POM/PEO blend higher than that of pure POM. At present, it is a challenge to measure the viscosity of polymer blend under the extremely high shear rate in microinjection molding process, which needs the further study. Finally, it is noteworthy that the POM spherulite size in the core layer decreased significantly with the addition of PEO. This phenomenon can be attributed to the inclusion or entanglement between POM and PEO molecules, which possibly interfered in the crystallization of POM and therefore reduced the size of spherulites.[14,19]

As stated earlier, the distribution of different polymer layers and their morphological state would influence the mechanical behavior of the microinjection molded components to a considerable degree. The morphology differences between the POM and POM/PEO microparts may lead to their different mechanical properties. It was found in many studies[23,26,27] that the orientation region occurring in the injection molded parts was proved to have remarkably enhancing effects on mechanical properties, e.g., the tensile strength, Young's modulus and impact toughness increased with increase in the thickness of the oriented region.[23,26] As shown in Figure 3, the thickness of the oriented region in POM/PEO micropart (86 μm) was close to

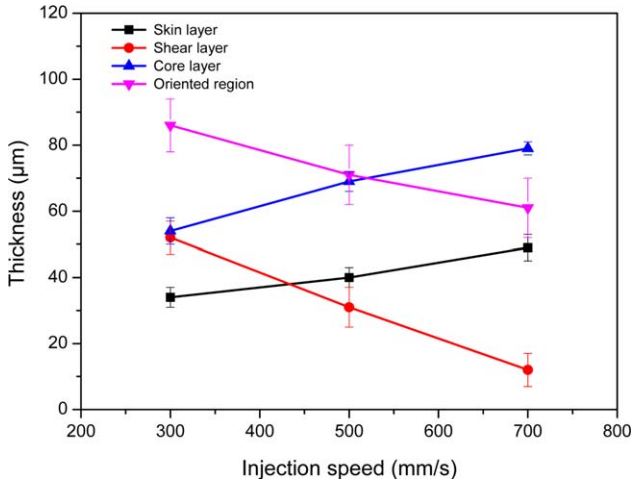

Figure 8. Effect of injection speed on the thicknesses of the different layers of the POM/PEO microparts. [Color figure can be viewed in the online issue, which is available at wileyonlinelibrary.com.]

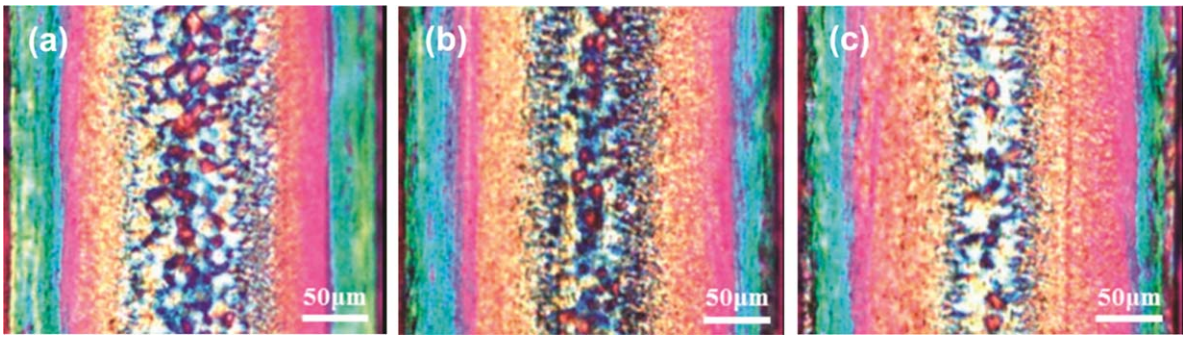

Figure 9. Polarized light micrographs of the full cross-sections of the POM/PEO microparts prepared at different mold temperatures: (a) 30°C, (b) 50°C, and (c) 70°C. [Color figure can be viewed in the online issue, which is available at wileyonlinelibrary.com.]

that in pure POM micropart (83 μm). As a result, it can be reasonably believed that the effect of the variation in thickness of the oriented region due to the presence of PEO on the mechanical properties of the POM/PEO micropart might be small.

The melting behaviors of pure POM and POM/PEO microparts were investigated by DSC in order to evaluate the effect of PEO on the crystallization behavior of POM in μIM. The DSC heating curves of pure POM and POM/PEO microparts are presented in Figure 5. The melting point T_m and the crystallinity X_c of POM and PEO are summarized in Table II. Considering the low PEO content, the corresponding DSC measurement for each sample was repeated 5 times. The obtained DSC parameters (T_m and X_c) were relatively stable and the standard deviations were in the range of 0.2–0.4%. For pure POM, a single and narrow endothermic melting peak at 164.8°C was observed on the DSC curve and a melting enthalpy $\triangle H_m$ of 161.3 J g^{-1} and a crystallinity X_c of 50.7% were obtained. It is interesting to observe that both the melting point ($T_{m\text{-POM}}$) and the crystallinity ($X_{c\text{-POM}}$) of POM reduced with addition of PEO, as shown in Table II. In addition, a small endothermic peak at around 60°C (indicated by the arrow) was also noticed on the heating curve of POM/PEO micropart, which should correspond to the melting endotherm of PEO domains in the blend.[14] It is believed that the special interactions between POM and PEO molecules mentioned previously can interfere in the crystallization of POM, resulting in the formation of some imperfect crystals with defects, as seen in Figure 6. This agrees with the results of Gao et al.,[14] who found PEO can interfere in the crystallization of POM to produce some disfigured crystals in conventional injection molding. Consequently, both the perfection level of POM crystals and the crystallinity $X_{c\text{-POM}}$ decreased with the introduction of PEO.

To have a deep knowledge of the crystalline and phase morphologies of POM/PEO micropart, which cannot be identified very clearly in PLM observations, the HFIP solution was used to etch the different layers of the POM/PEO micropart so as to remove the PEO particles and the amorphous phase of POM. The etched samples were observed using SEM. The results are shown in Figure 6. It can be seen that the spherulite structure of POM in the core layer can be observed more clearly after etching [Figure 6(b) vs. 6(c)]. In addition, the PEO domains (indicated by the arrow) were found to be embedded in the POM crystals. The size and distribution of the PEO domains were in good agreement with the results of PLM observations [Figure 2(a)]. There were many POM spherulites with diameters in the range of 7–10 μm found in the core layer, as shown in Figure 6(c), which were much smaller than the corresponding one (>80 μm) in conventional injection molding due to the confined space of microcavity.[14] Meanwhile, the highly oriented shish-kebab structures along the melt flow direction can be observed in the shear layers, as shown in Figure 6(d,e), respectively. This is consistent with those occurring in literature,[28] which found the shish-kebab structures of POM sample prepared by conventional injection molding. In addition, some oriented structures can also be observed in the skin layers, as shown in Figure 6(a), which were different from the shish-kebab structures in the shear layers. However, the difference in the oriented structures between skin layer and shear layer is that the former has no shish structure and the latter has. The reason for this can be illustrated as follows: during the microinjection molding process, when the molten polymer is injected into a mold, the polymer melt would contact the cold mold wall and instantly form a layer of solidified material (skin layer). The formation of such a skin layer will surely reduce the flow cross-sectional area and promote the thermal insulating barrier formation for the central molten polymer, leading to an increase

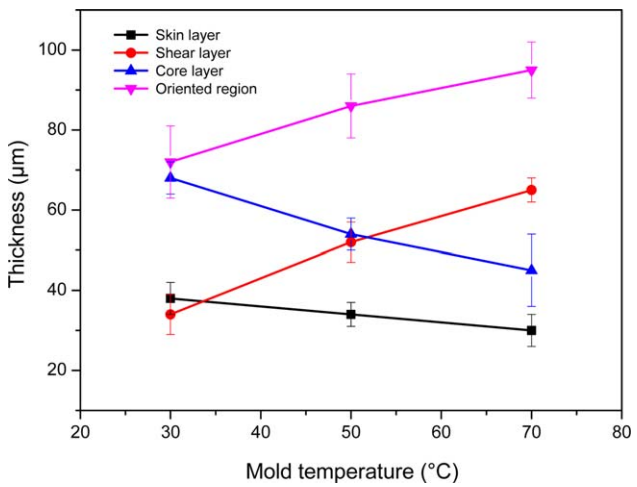

Figure 10. Effect of mold temperature on the thicknesses of the different layers of the POM/PEO microparts. [Color figure can be viewed in the online issue, which is available at wileyonlinelibrary.com.]

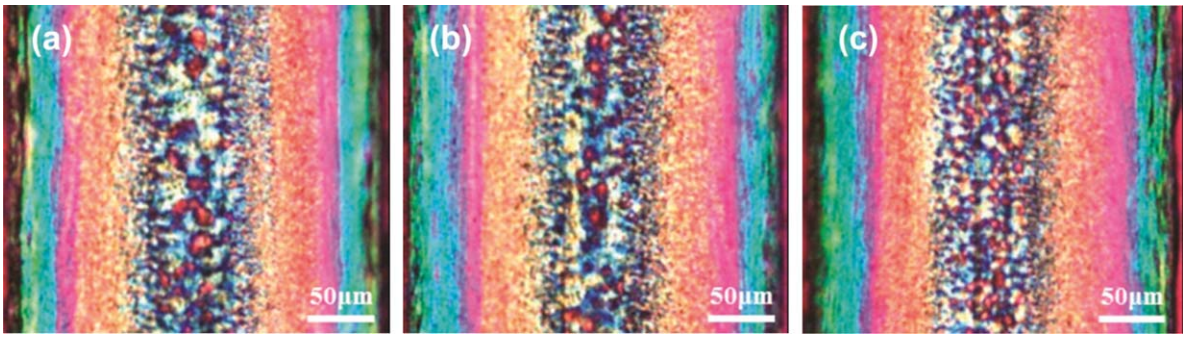

Figure 11. Polarized light micrographs of the full cross-sections of the POM/PEO microparts prepared under different injection pressures: (a) 150 MPa, (b) 200 MPa, and (c) 250 MPa. [Color figure can be viewed in the online issue, which is available at wileyonlinelibrary.com.]

in the shear stresses and a decrease in the cooling rates. These effects favor the flow-induced crystallization, in particular the formation of highly oriented lamellar structures in the shear layer. The shear stress imposed on polymer melt makes the molecules stretched along the direction of the shear field and form oriented structures (microfibrils or shish). The oriented structures parallel to the flow direction can promote the epitaxial growth of the layer-like structures (kebabs) perpendicular to the flow, resulting in formation of the shish-kebab structures in the shear layer.[5] However, in the skin layer region, the polymer melt would be instantly solidified near the cold mold and there is no time for the oriented macromolecular chains along the flow direction to crystallize to form the shish structure due to the extremely rapid cooling process.

Effect of Microprocessing Parameters on Crystalline Morphology

Figure 7 shows the polarized light micrographs of the POM/PEO microparts prepared at different injection speeds. It can be seen that the most obvious morphological difference between the microparts lies in the thicknesses of the different layers. To investigate the effect of microprocessing conditions on the morphology quantitatively, the average values and standard deviations of the measured thicknesses of the different layers of POM/PEO microparts with different injection speeds are shown in Figure 8. As can be seen, with increasing the injection speed from 300 to 700 mm s^{-1}, the thicknesses of the shear layer and the oriented region decreased significantly, while that of the skin layer increased slightly, and the core thickness increased obviously. The increase in the injection speed would lead to the increase in the shear stress in the polymer melt near the cavity wall. In this way, the skin layer would become thicker. However, the increase in the injection speed also decreased the melt filling time and, consequently, the time that the polymer melt experienced flow stress decreased, which would result in the reduction in the shear layer thickness.[23]

The PLM images of the POM/PEO microparts prepared at different mold temperatures are presented in Figure 9. Figure 10 shows a quantitative indication of the variation of the thicknesses of the different layers of the POM/PEO microparts with mold temperature. As can be interestingly seen, with increasing the mold temperature from 30 to 70°C, there were different changes in the thicknesses of different layers of POM/PEO microparts. For the skin layer, the thickness showed a slightly decreasing tendency. However, there was a remarkable increase in the thickness of shear layer and a remarkable decrease in the thickness of core layer instead. Because of the significantly increased thickness of the shear layer, the oriented region, of course, would show an obviously increasing tendency in the thickness. It is believed that at a higher mold temperature, a longer time is needed to reach the freezing point of the polymer melt near the mold wall. Undoubtedly, the thickness of the skin layer would decrease. The change of the thickness of the shear layer with the mold temperature can be explained by the following analysis: although the orientation of the molecular chains depends on the competition between the stress-induced orientation and the subsequent molecular relaxation, the samples were subjected to much stronger stress during microinjection molding than during convention injection molding, therefore the extended level of the molecular chains was higher and their resistance to disorientation was stronger, and the effect of the cooling rate on the molecular relaxation was smaller. Moreover, the decrease in the cooling rate caused by higher mold temperature would increase the crystallization temperature,[10] which was favorable to the growth of shish-kebab morphology, i.e., a thickened shear layer. On the other hand, the decreased skin layer would make

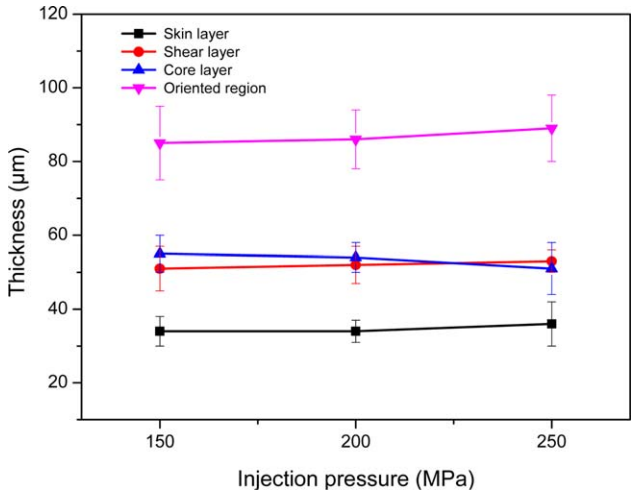

Figure 12. Effect of injection pressure on the thicknesses of the different layers of the POM/PEO microparts. [Color figure can be viewed in the online issue, which is available at wileyonlinelibrary.com.]

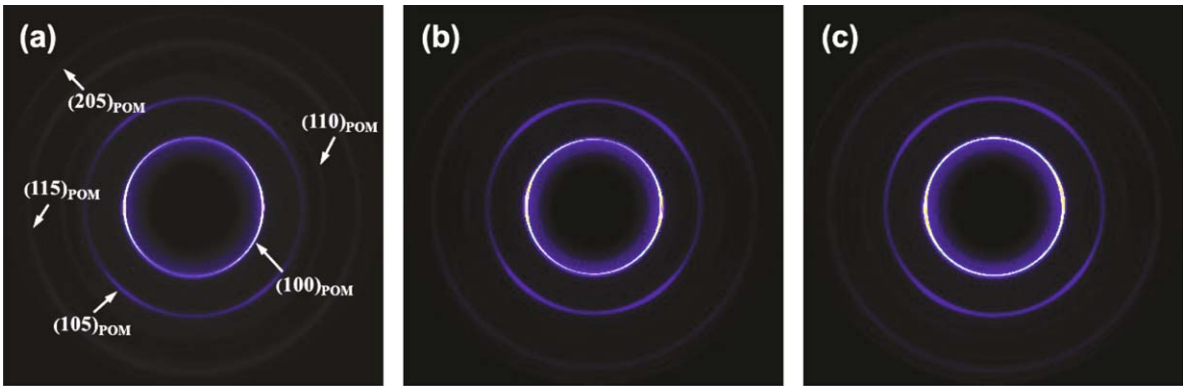

Figure 13. Two-dimensional WAXD patterns of POM/PEO microparts prepared at different injection speeds: (a) 300 mm s^{-1}, (b) 500 mm s^{-1}, and (c) 700 mm s^{-1}. The flow direction is vertical. [Color figure can be viewed in the online issue, which is available at wileyonlinelibrary.com.]

the melt have more filling time. This would surely prolong the time for the polymer melt to suffer the flow shear stress and hence would increase the possibility of the stress-induced orientation of polymer molecular chains in molten state, which, of course, favors the formation of the thicker shear layer. As a result, the shear layer thickness increased with the increase in the mold temperature. It is also noted that both the number and the size of the spherulites in the core layer decreased with increasing the mold temperature. The reduction in the spherulite number could be attributed to the lower nucleation rate caused by the higher bulk temperature in the core layer. However, the decrease in the spherulite size with increasing mold temperature is contrary to the normal result, which is interesting and needs to be further investigated. At the current stage, it is believed that the interactions between POM and PEO molecules, as mentioned previously, may be enhanced with increase of mold temperature due to the enhanced thermal movement of molecular chains (the probability of the chain inclusion and entanglement increased), which would interfere in the POM crystallization to a more considerable extent and consequently would lead to the formation of the smaller spherulites.

The polarized light micrographs of POM/PEO microparts prepared under different injection pressures are shown in Figure 11. Figure 12 displays the variation of the thicknesses of the different layers of the POM/PEO micropart with the injection pressure quantitatively. It is seen that the thicknesses of the different layers under different injection pressures were similar, suggesting that the injection pressure had small effect on the development of the thicknesses of different layers for POM/PEO micropart. It is further noted that with increasing the injection pressure, the number of the spherulite in the core layer increased and however the size of the spherulite decreased. This is probably due to the increase in the nucleation rate in the core layer under the enhanced injection pressure.

So far, we have investigated the influences of three microprocessing factors, including injection speed, mold temperature and injection pressure, on the crystalline morphology of POM/PEO micropart. Both injection speed and mold temperature were

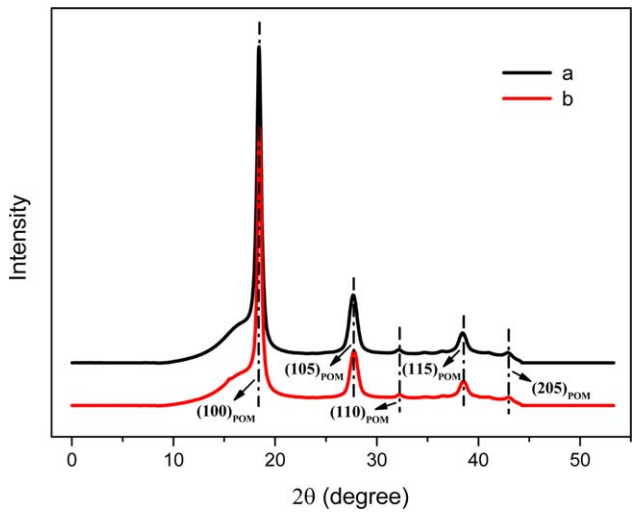

Figure 14. The 1D-WAXD curves of the POM (a) and POM/PEO (b) microparts microinjection molded under the same microprocessing conditions (injection speed: 300 mm s^{-1}; mold temperature: 50°C; injection pressure: 200 MPa). [Color figure can be viewed in the online issue, which is available at wileyonlinelibrary.com.]

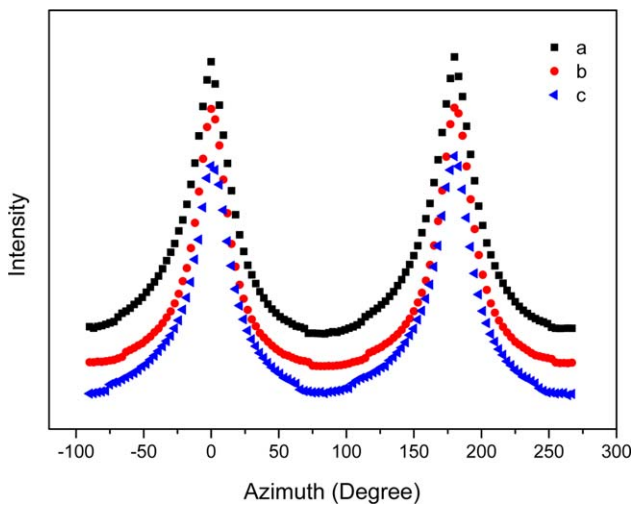

Figure 15. The azimuthal profiles of (100) reflection of POM/PEO microparts prepared at different injection speeds: (a) 300 mm s^{-1}, (b) 500 mm s^{-1} and (c) 700 mm s^{-1}. [Color figure can be viewed in the online issue, which is available at wileyonlinelibrary.com.]

Table III. The Orientation Parameter f Estimated from Azimuthal Intensity Curve of (100) Reflection of the POM/PEO Microparts with Different Processing Parameters

Sample series	Micro processing parameters		
A	Injection speed		
	300 (mm s^{-1})	500 (mm s^{-1})	700 (mm s^{-1})
	0.2552	0.2204	0.1770
B	Mold temperature		
	30 (°C)	50 (°C)	70 (°C)
	0.2354	0.2552	0.3094
C	Injection pressure		
	150 (MPa)	200 (MPa)	250 (MPa)
	0.2518	0.2552	0.2579

found to have pronounced influence on the crystalline morphology development of POM/PEO micropart, while the effect of injection pressure was relatively small, which are quite different from the published results of the conventional injection molding, because injection pressure is the primary control variable for conventional injection molding machines.[29]

It should be pointed out that the thickness of the oriented region has a significant effect on the mechanical properties of POM/PEO micropart. The optimization of microprocessing conditions would lead to formation of larger fraction of the oriented structures. Consequently, this could be important for tuning the microstructure so as to achieve the desired product properties to a certain degree.

Effect of Microprocessing Parameters on Crystalline Orientation

As indicated by the PLM observations, the microprocessing parameters had remarkable effect on the morphology development of POM/PEO micropart. So, it is important to clarify the polymer crystalline orientation. Here, the crystalline orientation in POM/PEO microparts prepared under different microprocessing conditions was further investigated by 2D-WAXD measurements.

Figure 13 shows the 2D-WAXD images of POM/PEO microparts prepared at different injection speeds. The 1D-WAXD curves [corresponding to Figure 13(a)] are also provided in Figure 14. Combining the 2D-WAXD with the 1D-WAXD results, the orientation of the crystal planes related to the orientation of polymer chains within lamellae can be reliably evaluated. As can be seen, the reflections in the 2D-WAXD patterns of the POM/PEO microparts from inner to outward could be assigned to (100), (105), (110), (115), and (205) crystal planes of hexagonal crystal of POM, corresponding to the 2θ value of 18.4°, 27.7°, 32.2°, 38.5°, and 43.0° in the 1D-WAXD patterns, respectively.[30] In addition, the 1D-WAXD curve of POM/PEO micropart was almost the same as that of POM micropart except for the intensity and there were not any reflections of PEO found. This indicated that the amount of crystalline PEO that is sufficiently ordered to give rise to reflections is too small to be identified, probably due to the low PEO content (5 wt %) and the tiny size (<2 μm) of the well dispersed PEO droplets in POM matrix. Because of the confined space, a smaller droplet will crystallize more slowly than a larger one, obeying the Evans–Avrami law.[31] The smaller the nodule, the slower the transformation. When the crystallization kinetics becomes slower than the extreme rapid cooling rate under microinjection molding conditions, the so small droplets may not or only partially crystallize, thus causing the amount of the sufficiently ordered PEO crystal to decrease.[32] From Figure 13, it can be also seen that the (100) reflection appeared as two distinguishable arcs at the equator and the (105) reflection appeared as four distinguishable arcs at the outer ring. This indicates that there was structure orientation occurring in the POM/PEO micropart. Figure 15 shows the dependence of reflection intensity on the azimuth angle from −90° to 270°, where 0° represents the equatorial direction. It can be seen that with decreasing injection speed, the azimuthal peak width gradually decreased. This can be ascribed to the development of the oriented structures in the micropart, indicating a noticeable orientation of POM macromolecular chains within lamellae in micropart.

The Herman's orientation function can be applied to quantitatively evaluate the orientation level of various planes, based on the following two equations[9]:

$$f = \frac{3\langle\cos^2\varphi\rangle - 1}{2} \tag{1}$$

$$\langle\cos^2\varphi\rangle = \frac{\int_0^{\pi/2} I(\varphi)\sin\varphi\cos^2\varphi\,\mathrm{d}\varphi}{\int_0^{\pi/2} I(\varphi)\sin\varphi\,\mathrm{d}\varphi} \tag{2}$$

where φ is the angle between the normal of a given crystal plane and melt shear flow direction and I is the intensity. Just taking $\varphi = 0$ as the shear flow direction, the limiting values of the orientation parameter f can be obtained: −0.5 for a

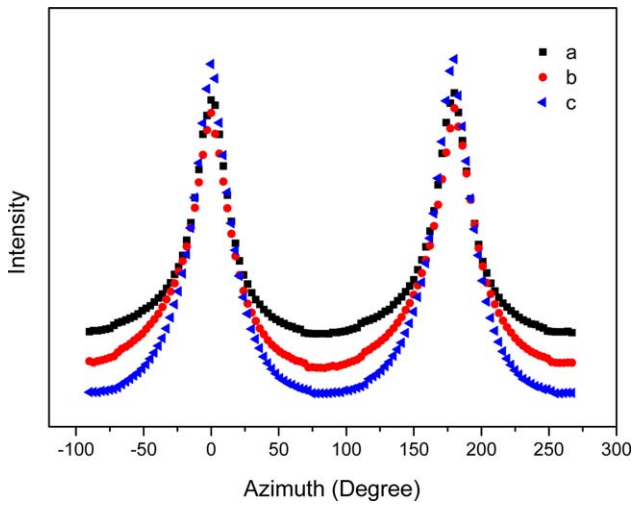

Figure 16. The azimuthal profiles of (100) reflection of POM/PEO microparts prepared at different mold temperatures: (a) 30°C, (b) 50°C, and (c) 70°C. [Color figure can be viewed in the online issue, which is available at wileyonlinelibrary.com.]

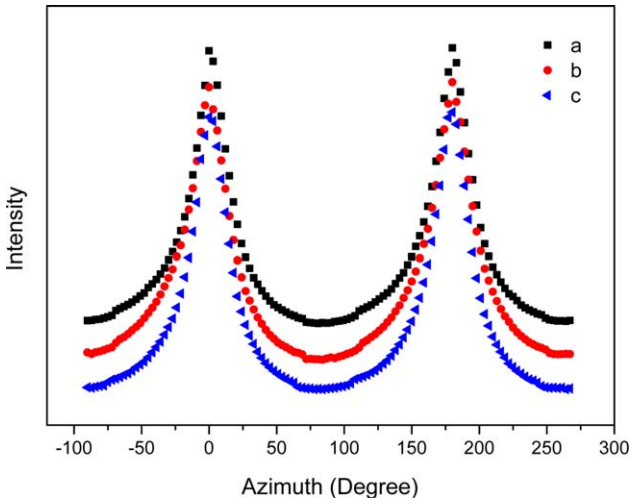

Figure 17. The azimuthal profiles of (100) reflection of POM/PEO microparts prepared under different injection pressures: (a) 150 MPa, (b) 200 MPa, and (c) 250 MPa. [Color figure can be viewed in the online issue, which is available at wileyonlinelibrary.com.]

perfectly perpendicular orientation and 1.0 for a perfectly parallel orientation. A randomly oriented sample gives $f = 0$.

The (100) reflection of hexagonal crystal of POM in this study was chosen to quantitatively evaluate the orientation level of the micropart. The orientation parameters estimated from the azimuthal intensity curves of (100) reflection of the POM/PEO microparts with different injection speeds are listed in Table III. For the purpose of easy comparison, the corresponding orientation parameters obtained at the other microprocessing parameters (mold temperature and injection pressure) to be investigated later are also included in Table III. It can be seen that with increasing the injection speed (sample series A), the orientation parameter reduced obviously, suggesting that injection speed had pronounced influence on the crystalline orientation in the microparts. This is in agreement with the results of the PLM observations (Figures 7 and 8). The 2D-WAXD images were taken with the beam irradiating the samples across the full thickness along the ND direction and therefore can be representative of the average morphology of the samples. Compared with other polymeric material such as polypropylene,[9] the fraction of core layer in the total POM/PEO micropart system is much larger. Therefore, the absolute values of the orientation parameters of POM/PEO microparts prepared at different processing parameters were comparatively small in this article.

For the influence of mold temperature, the corresponding azimuthal intensity curves of (100) reflection of POM/PEO microparts are shown in Figure 16. As can be seen, with increasing the mold temperature, the azimuthal peak width gradually became narrow, suggesting that the orientation of polymer macromolecular chains within lamellae became more pronounced. The result can be confirmed by the orientation parameters of micropart samples prepared at different mold temperatures (Table III). From Table III, it can be seen that an increase in mold temperature (sample series B) resulted in a higher orientation parameter. Combined with the PLM analysis mentioned previously, it can be concluded that the thickness of the oriented region was positively correlated with the orientation parameter, while the thickness of the core layer was negatively correlated with the orientation parameter.

The influence of the injection pressure was also investigated. The obtained results are shown in Figure 17. Combined with Table III, it can be seen that with increase in injection pressure (sample series C), the differences in the values of the orientation parameters estimated from the corresponding azimuthal intensity curves of (100) reflection (Figure 17) were not remarkable, indicating that the injection pressure had small influence on the crystalline orientation in POM/PEO microparts. This means that the orientation of polymer macromolecular chains within lamellae cannot be manipulated effectively by only changing injection pressure.

CONCLUSIONS

To manufacture a POM-based micropart (e.g., microgear) with good comprehensive performances, the microinjection molding was first conducted on the POM/PEO blend system. The introduction of PEO was expected to impart a good impact resistance and self-lubricity to the POM-based micropart based on our previous studies. The optical, thermal and X-ray diffraction measurements were used to characterize the crystalline behavior and orientation of the POM/PEO blend microparts prepared under different microprocessing conditions, including injection speed, mold temperature, and injection pressure. To clarify the effect of the incorporated PEO in the POM/PEO blend micropart, the comparison was also carried out between pure POM and POM/PEO blend microparts. Based on above characterizations and discussions, the following conclusions can be obtained.

1. In both POM and POM/PEO microparts, a typical skin-core structure was identified. Compared to POM micropart, the POM/PEO micropart showed thicker shear layer but thinner skin layer and core layer. PEO was uniformly dispersed in POM matrix. There were shish-kebab orientation structures observed in the shear layers of the POM/PEO microparts. Compared with POM micropart, the spherulite size, the melting point and the crystallinity of POM in the POM/PEO micropart decreased, which is attributed to the specific interactions between POM and PEO molecules.
2. The microprocessing conditions, including injection speed, mold temperature, and injection pressure, showed a complicated influence on the thicknesses of different layers in the POM/PEO microparts. With increase in the injection speed or decrease in the mold temperature, the thicknesses of the skin layer and the core layer increased, while the thicknesses of the shear layer and the oriented region decreased. The influence of the injection pressure was not obvious.
3. Based on the 2D-WAXD and also the 1D-WAXD results, the microprocessing conditions also affected the crystalline orientation of POM/PEO microparts, which is important for realization of the high performance of the micropart. The increase in the injection speed or decrease in the mold

temperature led to the reduction of orientation parameter *f*, i.e., the degree of orientation decreased. The influence of the injection pressure on the orientation parameter *f* (crystalline orientation) was also very limited.

ACKNOWLEDGMENTS

This work was financially supported by the National Natural Science Foundation of China (Grant No. 51010004), the Programme of Introducing Talents of Discipline to Universities (Grant No. B13040), the Foundation for Innovative Research Groups of the National Natural Science Foundation of China (Grant No. 51121001) and International Science and Technology Cooperation Program of China (Grant No. 2010DFA54460). The authors are deeply indebted to the Shanghai Synchrotron Radiation Facility (SSRF) and Prof. Jie Wang (SSRF) for his help in synchrotron WAXD measurements.

REFERENCES

1. Piotter, V.; Mueller, K.; Plewa, K.; Ruprecht, R.; Hausselt, J. *Microsyst. Technol.* **2002**, *8*, 387.
2. Kukla, C.; Loibl, H.; Detter, H. *Kunstst.-Plast. Eur.* **1998**, *88*, 1331.
3. Zauner, R. *Microelectron. Eng.* **2006**, *83*, 1442.
4. Chien, R. D.; Jong, W. R.; Chen, S. C. *J. Micromech. Microeng.* **2005**, *15*, 1389.
5. Giboz, J.; Copponnex, T.; Mele, P. *J. Micromech. Microeng.* **2009**, *19*, 025023.
6. Yao, D.; Kim, B. *J. Micromech. Microeng.* **2002**, *12*, 604.
7. Zhang, J.; Guo, C.; Wu, X.; Liu, F.; Qian, X. *J. Macromol. Sci. B* **2011**, *50*, 2227.
8. Lu, Z.; Zhang, K. F. *Polym. Eng. Sci.* **2009**, *49*, 1661.
9. Liu, F.; Guo, C.; Wu, X.; Qian, X.; Liu, H.; Zhang, J. *Polym. Adv. Technol.* **2012**, *23*, 686.
10. Viana, J. C. *Polymer* **2004**, *45*, 993.
11. Liou, A. C.; Chen, R. H. *Int. J. Adv. Manuf. Tech.* **2006**, *28*, 1097.
12. Sha, B.; Dimov, S.; Griffiths, C.; Packianather, M. S. *J. Mater. Process. Tech.* **2007**, *183*, 284.
13. Laursen, J. L.; Sivebaek, I. M.; Christoffersen, L. W.; Papsoee, M.; Vigild, M. E.; Brondsted, P.; Horsewell, A. *Wear* **2009**, *267*, 2294.
14. Gao, Y.; Sun, S.; He, Y.; Wang, X.; Wu, D. *Compos. Part B Eng.* **2011**, *42*, 1945.
15. Bai, S. B.; Liu, J. L.; Wang, Q. *China Plast.* **2007**, *21*, 67.
16. Bai, S. B.; Liu, J. L.; Wang, Q. *Polym. Mater. Sci. Eng.* **2007**, *23*, 136.
17. Bai, S. B. Formation and Control of Multi-scale Crystalline Structure in POM/PEO Crystalline/Crystalline Blends with High Performances. Ph.D. Thesis, Sichuan University, Chengdu, China, June **2007**.
18. Liu, X.; Bai, S. B.; Nie, M.; Wang, Q. *J. Polym. Res.* **2011**, *19*, 1.
19. Liu, X.; Bai, S. B.; Wang, Q. *J. Macromol. Sci. B* **2011**, *51*, 642.
20. Huang, C. K. *Eur. Polym. J.* **2006**, *42*, 2174.
21. Abbasi, S.; Derdouri, A.; Carreau, P. J. *Polym. Eng. Sci.* **2011**, *51*, 992.
22. Xie, L.; Ziegmann, G. *J. Alloy Compd.* **2011**, *509*, 226.
23. Schrauwen, B. A. G.; Breemen, L. C. A. V.; Spoelstra, A. B.; Govaert, L. E.; Peters, G. W. M.; Meijer, H. E. H. *Macromolecules* **2004**, *37*, 8618.
24. Iguchi, M. *Die Makromol. Chem.* **1976**, *177*, 549.
25. Wunderlich, B. Macromolecular Physics; Academic Press: New York, **1980**; Vol. *3*, Chapter 8, p 66.
26. Kalay, G.; Sousa, R. A.; Reis, R. L.; Cunha, A. M.; Bevis, M. J. *J. Appl. Polym. Sci.* **1999**, *73*, 2473.
27. Kantz, M. R.; Newman, H. D.; Stigale, F. H. *J. Appl. Polym. Sci.* **1972**, *16*, 1249.
28. Kawaguchi, K. *J. Appl. Polym. Sci.* **2006**, *100*, 3382.
29. Kamal, M. R.; Chu, J.; Derdouri, S.; Hrymak, A. *Plast. Rubber Compos.* **2010**, *39*, 332.
30. Carazzolo, G. A. *J. Polym. Sci. Part A: Polym. Chem.* **1963**, *1*, 1573.
31. Avrami, M. *J. Chem. Phys.* **1940**, *8*, 212.
32. Everaert, V.; Groeninckx, G.; Koch, M. H. J.; Reynaers, H. *Polymer* **2003**, *44*, 3491.